

RESEARCH PAPER

## Enhancing Properties of Polyvinyl Alcohol Film using Sorghum Starch Nanocrystals

S. Vasantha Kumar, V.A. Sajeevkumar\*, Johnsy George, and Sunny Kumar

Food Engineering and Packaging Division, Defence Food Research Laboratory, Mysuru- 570 011, India

\*E-mail: va.sajeevkumar@dfri.drdo.in

### ABSTRACT

Polyvinyl alcohol (PVA) nanocomposite films with sorghum starch nanocrystals (SSN) were prepared by incorporating various concentrations of SSN in PVA. SSN was isolated using acid hydrolysis of sorghum starch. The morphological studies of SSN using atomic force microscopy (AFM) revealed that the particle size varied from 65 nm to 68 nm. The mechanical properties of PVA-SSN nanocomposite films indicated an improvement in tensile strength and percentage elongation at break when compared to that of PVA films. This can be attributed to the stronger interaction of PVA with SSN due to hydrogen bonding. Besides this, PVA-SSN nanocomposite films also exhibited good thermal properties. Thus, the use of SSN imparted superior properties to the PVA nanocomposite films, which will be beneficial for applications such as food packaging.

**Keywords:** Polyvinyl alcohol; Sorghum starch; Nanocrystals; FTIR; Physico - mechanical; Thermal properties

### NOMENCLATURE

PVA	Polyvinyl alcohol
SS	Sorghum starch
SSN	Sorghum starch nanocrystals
FTIR	Fourier transform infrared
SEM	Scanning electron microscopy
AFM	Atomic force microscopy
XRD	X-ray diffractometer
UTM	Universal testing machine
DSC	Differential scanning calorimeter
TGA	Thermogravimetric analysis
DMA	Dynamic mechanical analysis

### 1. INTRODUCTION

Polyvinyl alcohol (PVA) is a synthetic water-soluble, commodity polymer with good mechanical and thermal properties. It has good film forming abilities and widely used in a variety of industries such as textile, paint, adhesive, coating industry, etc throughout the world<sup>1</sup>. Properties of PVA which makes it versatile with many industrial and biomedical applications are its better physical properties, biocompatibility, chemical resistance, good thermal stability, strong adhesion, etc<sup>2</sup>. Although PVA is having reasonably good properties, there has been considerable amount of interest among researchers in the development of composites of PVA by blending with fillers especially naturally occurring polymers to improve its thermal and mechanical properties, processability, as well as biodegradation capability even in anaerobic conditions. Common polymeric fillers used for blending with PVA are

natural polymers like starch<sup>3,4</sup>, cellulose<sup>5</sup>, chitosan<sup>6</sup>, proteins<sup>7</sup>, etc. But the composite films formed after blending of PVA with other materials has shown to decrease its physico - mechanical properties, thermal properties and even film forming characteristics due to poor compatibility between PVA and the added fillers<sup>4</sup>. The advent of nanomaterials opened a new path to almost all field of science due to its structural features as well as special properties at nanoscale. They are also having large surface area with respect to mass ratios due to their small size, leading to high filler connectivity and small interparticle separation when dispersed in a polymer matrix compared to larger fillers<sup>8</sup>. These properties of nanomaterials attracted the attention of researchers in recent years and various PVA nanocomposites have been developed by incorporation of several nanomaterials as fillers in the polymer matrix. Some of the nanomaterials which were used as nanofillers in PVA include carbon nanotubes (CNT)<sup>9</sup>, graphene<sup>10</sup>, functionalised carbon nanotubes<sup>11</sup>, nanoclays<sup>12</sup>, etc. The improvements in properties of polymer nanocomposites is dependent on the size, shape, aspect ratio, modulus, structural and morphological properties of the nanoparticles as well as uniform dispersion, alignment and interaction of the nanomaterial with the matrix in the nanocomposite.

PVA nanocomposite materials containing inorganic materials such as montmorillonite clay have been reported. It has better potential in commercial application as a result of its good thermal, mechanical as well as barrier properties even at lower levels of clay loading<sup>13</sup>. Development of such nanocomposites involves application of high shear force for uniform dispersion and exfoliation of the clay material in the polymer matrix to get desired properties. However, environmental concerns have forced researchers to focus on bio-based nanomaterials

which could be derived from polysaccharides, in place of nanoclays and nanocarbon. Moreover, the naturally occurring crystalline nanomaterials such as cellulose nanocrystals from plant and bacterial sources as well as starch nanocrystals are better suitable for blending with PVA as both being polar, can have better interaction (including hydrogen bonding) between them, resulting in better system integrity, stability and properties. PVA nanocomposites containing naturally occurring nanomaterials such as peas starch nanocrystals<sup>14</sup> and cellulose nanocrystals<sup>15</sup>, has been reported to have enhanced the properties of the nanocomposites obtained.

Sorghum is a cereal obtained from maize like grass native to Africa and Asia and utilised as a source of food, feed, and fuel<sup>16</sup>. The sorghum grains is the staple food for a large section of people in China, India and Africa. Sorghum which is the world fifth most important cereal has been found to have an average starch content ranging from 56 per cent to 73 per cent<sup>17</sup>. Like the starch from other cereals, sorghum starch also has two major molecular components, amylose and amylopectin. Most of the genotype contains amylose at around 20 per cent to 30 per cent. The amylopectin in sorghum starch has been reported to have double helical structure which is mostly further crystallised into granules<sup>18</sup>. Sorghum starch from kernals has been reported to have 'A' type x-ray polymorphs. The percentage of crystallinity has been reported to range from 22 per cent to 29 per cent<sup>19</sup>. The sorghum starch has been used for food as well as non-food purpose such as tablet formulation, substrate for bacteria, bio-fuel production, etc. Although literature indicates a few starch nanocrystals studies from different botanical origin<sup>14</sup>, to the best of our knowledge, the studies and application of sorghum starch nanocrystals in the development of polymer nanocomposite using polyvinyl alcohol is not available. Hence the present study involving extraction and characterisation of starch nanocrystals from sorghum starch followed by development and evaluation of polyvinyl alcohol starch nanocomposites have been undertaken with a view to develop more ecofriendly and cost effective packaging system for food contact applications.

## 2. MATERIALS AND METHODS

Sorghum grains were purchased from local market at Mysuru, Karnataka, India. Commercial grade sodium hydroxide (M.W = 40.0) and sulphuric acid (H<sub>2</sub>SO<sub>4</sub>) were procured from Sd fine Chemicals, India. PVA having a molecular weight of 14,000 was supplied by Fisher Scientific India.

### 2.1 Isolation of Sorghum Starch

Sorghum starch (SS) was isolated from sorghum grains using alkali method<sup>20</sup> by removing protein from it. Sorghum grains were powdered and the powder was then steepened in 0.2 per cent sodium hydroxide solution at room temperature for 24 h. The supernatant layer was decanted and the slurry was diluted to the original volume with more sodium hydroxide solution. The process was repeated until the supernatant becomes clear and gives a negative reaction to the Bi-uret test for protein. The SS thus obtained was suspended in distilled water, passed through 100-200 mesh nylon cloth and repeatedly washed with water until pH of the supernatant was around 7.0 measured

using a pH meter. (Eutech Instruments, Thermo Fisher Scientific, India). The SS was collected by centrifugation and later dried in an incubator (Appolo Scientific Surgicals co, India) at 40 °C. The total yield of SS obtained was around 78-80 w/w per cent.

### 2.2 Preparation of Sorghum Starch Nanocrystals

Sorghum starch nanocrystals (SSN) were prepared by following the method previously reported for waxy maize starch<sup>21</sup>. 15 g of SS was mixed with 100 ml of 3.14 M sulphuric acid solution in a round bottom flask. The suspension was maintained at 40 °C and stirred continuously at 180 rpm in an orbital shaker (Scigenics Biotech Pvt Ltd, India). After five days of acid hydrolysis, the suspensions was centrifuged. The precipitate was repeatedly washed with distilled water and centrifuged each time (Remi Elektrotechnik Ltd., India) until the suspension was neutral (confirmed using a pH meter). This resultant residue was lyophilised to get a fine powder of SSN.

### 2.3 Preparation of PVA Nanocomposite Films

PVA solution was prepared by dissolving 10 g PVA in 100 ml distilled water at 90 °C for 4 h with mechanical stirring. Different weight percentage of SS and SSN (2 to 12 wt per cent) were dispersed in a known weight of PVA solution. The solution was casted on a flat, levelled, non sticky polymer surface and allowed to dry at room temperature to obtain films of uniform thickness. The films, after vacuum drying at 40 °C, were kept in a desiccator containing P<sub>2</sub>O<sub>5</sub> before it was used for further analysis. All the films were conditioned at 50 Per cent RH for 7 days and were used for mechanical and thermal properties evaluation.

### 2.4 Fourier Transform Infrared Spectroscopic Analysis

Infra red spectra of all the samples were recorded using Thermo Nicolet FTIR Spectrometer (Model 5700), Madison, WI, USA using single bounce ATR accessory having Zinc Selenide crystal. All the spectra were recorded in the mid IR range at 4 cm<sup>-1</sup> resolution. 32 scans were averaged to get the IR spectra. FTIR spectra of some samples were measured in the absorbance mode also from 4000 cm<sup>-1</sup> – 400 cm<sup>-1</sup> with the same resolution for the examination of low intensity bands.

### 2.5 Morphological Characterisation

Morphological analysis of SS and SSN were carried out using Scanning Electron Microscopy (SEM) (CARL Zeiss, EVO LS 10, Germany) and Atomic Force Microscopy (Solver PRO NT-MDT, Ireland) respectively. For SEM analysis, samples were initially dried in vacuum and placed on an aluminium stub using double sided aluminium tape and sputter coated using gold to make it conductive. The morphological analysis was carried out at high vacuum using an operating voltage of 20 kV. For AFM analysis a small amount of SSN was dispersed in distilled water and a drop of the suspension was dried overnight on a freshly cleaved mica substrate. The images were acquired using non-contact mode with silicon cantilevers, having a tip curvature radius of 10 nm and a force constant of 1.45 N/m - 15.1 N/m.

## 2.6 XRD Analysis

The x-ray diffractograms (XRD) of the SS, SSN, and PVA nanocomposite films were recorded using Rigaku Miniflex - II (Japan) having Ni filter, CuK $\alpha$  radiation of wavelength  $\lambda=1.5406 \text{ \AA}$ , with a graphite monochromator. The samples were scanned in the  $2\theta$  range  $4^\circ$ - $40^\circ$  with a scan speed and step size of  $5^\circ/\text{min}$  and  $0.02$ , respectively.

## 2.7 Mechanical Properties

Mechanical properties of PVA and all its composites films were evaluated in tensile mode using Universal Testing Machine (UTM) (Lloyd Instruments, Model: LRX Plus), with a cross head speed of  $100 \text{ mm/min}$  and gauge length of  $1 \text{ inch}$ . All the samples were cut into strips of  $5 \text{ cm} \times 1 \text{ cm}$  and evaluation was carried out as per ASTM D882 method.

## 2.8 Differential Scanning Calorimetry

Differential Scanning Calorimeter (DSC) with a thermal analyst system (DSC 2910, TA Instrument, USA) was used to determine the glass transition temperature ( $T_g$ ), melting temperature ( $T_m$ ) and melting enthalpy ( $\Delta H_m$ ) of PVA and its nanocomposites films. Samples were scanned at a heating rate of  $10^\circ\text{C/min}$  over temperature range of  $-20^\circ\text{C}$  to  $250^\circ\text{C}$ .

## 2.9 Thermogravimetric Analysis

Thermogravimetric analysis (TGA) was carried out using TGA Q50 (TA instrument, USA) to determine the thermal stability of PVA and its nanocomposites under nitrogen flow rate of  $20 \text{ ml/min}$ . The samples were heated from  $30^\circ\text{C}$  to  $600^\circ\text{C}$  with a heating rate of  $10^\circ\text{C/min}$ . The onset, peak and completion temperature were calculated using software provided along with the instrument.

## 2.10 Dynamic Mechanical Analysis

Dynamic mechanical analysis was performed on a dynamic mechanical thermal analyser (Model Q 800, TA instrument, USA). Measurements were carried out by applying a constant shear stress at a frequency of  $5 \text{ Hz}$  while fixing the static load at  $4.0 \text{ N}$  and dynamic load at  $2.0 \text{ N}$  respectively. The samples of dimensions  $2 \text{ cm} \times 6 \text{ cm}$  was cut from the films and were tested at a temperature range of  $25^\circ\text{C}$  to  $80^\circ\text{C}$  by providing a heating rate of  $5^\circ\text{C/min}$ . The storage modulus and  $\tan \delta$  of the samples were measured.

## 3. RESULT AND DISCUSSION

### 3.1 FTIR Characterisation

FTIR spectra in the range  $1800 \text{ cm}^{-1}$  –  $650 \text{ cm}^{-1}$  of powdered sorghum grains, extracted sorghum starch and sorghum starch nanocrystals are given in Fig. 1. It is evident from the figure that sorghum powder is having a weak and broad band between  $1600 \text{ cm}^{-1}$  and  $1500 \text{ cm}^{-1}$  which corresponds to amide II band of proteins. The absence of this band in extracted SS indicates that the proteins have been completely removed from raw sorghum powder during alkali treatment. The broad

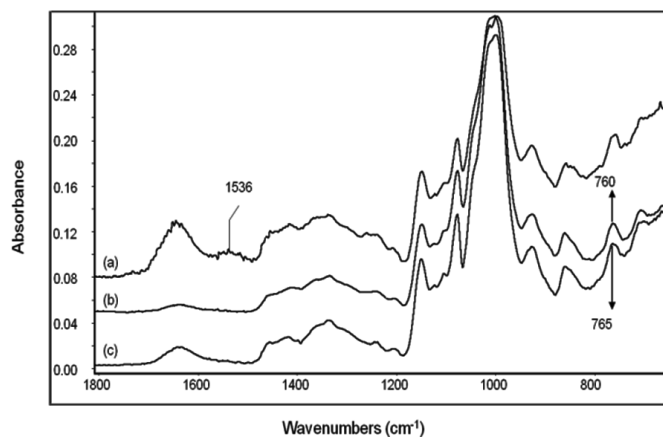


**Figure 1.** FTIR spectra of (a) raw sorghum powder, (b) sorghum starch, and (c) sorghum starch nanocrystals.

band appearing around  $1644 \text{ cm}^{-1}$  for raw sorghum powder can be assigned to bending vibration of bound water molecules in it. They exist through the hydrogen bonding interaction with starch as well as other polar contents such as proteins in it. As a result of these molecular interactions, this band is appearing at a higher frequency compared to that in SS. After the removal of proteins from raw sorghum powder during alkali treatment, the amount of bound water in the system reduces resulting in lower intensity of this band in SS. The low frequency shift of the band in SS in comparison to raw sorghum powder clearly indicates diminished molecular interaction between bound water and starch relative to that in raw sorghum powder. The band assignments for SS and SSN are tabulated in Table 1. It can be observed from Fig. 1 that the C-O-C ring vibration of the samples appears at  $760 \text{ cm}^{-1}$  and  $765 \text{ cm}^{-1}$  for SS and SSN, respectively. The high frequency shift of this mode of bending vibration is consistent with that reported in the case of pea starch and pea starch nanocrystals<sup>14</sup>. However, the IR absorption frequencies of the C-O-C ring vibration in the case of sorghum starch system were found to be slightly different from that of pea starch system. These bands were further used as characteristic frequency of SS and SSN in identification of the filler in PVA composites.

The FTIR spectra of PVA, PVA+10% SS and PVA+10% SSN composites films are presented in Fig. 2. The band assignments of prominent bands are provided

**Table 1.** Peak assignment in the FTIR spectra of raw sorghum powder, SS, SSN and PVA and its composites films

Peak assignment	Sorghum Powder	SS	SSN	PVA	PVA+SS	PVA+SSN
-OH (stretching)	3287	3256	3328	3281	3278	3274
C=O (stretching)	-----	-----	-----	1732	1734	1736
-OH (bending) of bound water	1644	1633	1640	1658	1654	1656
C-O (str) in C-O-H	1151	1148	1149	1139	1146	1147
C-O (stretching) in C-O-C	996	1074	1077	1094	1090	1088
C-O (bending) (c-o-c ring vibration in starch)	758	1003	1012	1046	1036	1028
		760	765	759	761	765

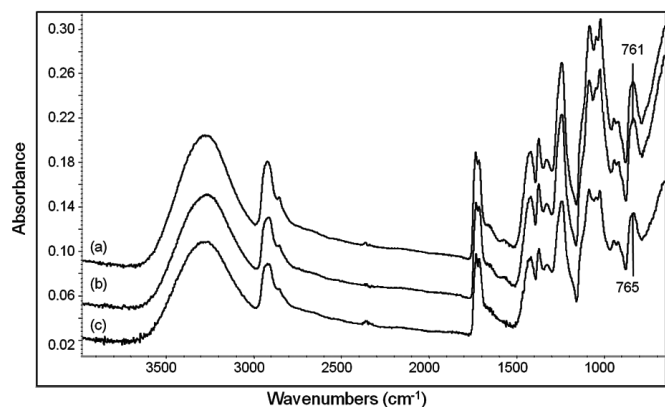


**Figure 2.** FTIR spectra of (a) PVA film, (b) PVA+10 % SS film and (c) PVA+10 % SSN film.

in Table 1. The appearance of characteristic starch band at  $761\text{ cm}^{-1}$  and  $765\text{ cm}^{-1}$  for PVA+10 % SS and PVA+10 % SSN systems respectively confirms the presence of SS and SSN in these systems. PVA has shown its characteristic absorption at  $1732\text{ cm}^{-1}$ , which were not overlapped by any other absorption peaks of sorghum starch. The two characteristic bands of PVA and sorghum starch co-existed in the FTIR spectra of the PVA+10 % SS and PVA+10 % SSN films confirming the presence of both the components in the composite material. On addition of SS to PVA, the peak position of  $-\text{OH}$  stretching band of PVA is showing a small low frequency shift. This indicates that there is an enhanced hydrogen bonding interactions between PVA and sorghum starch. The interaction is stronger between that of PVA and SSN as indicated by relatively larger low frequency shift of the  $-\text{OH}$  stretching band of PVA.

### 3.2 X-Ray Diffraction Analysis

In Fig. 3(a), SS shows the characteristic 'A' type crystalline pattern similar to that shown by other grains<sup>22</sup>. SS exhibited strong intensity peak at  $17.8^\circ$ ,  $23.1^\circ$  and two weak intensity peaks at  $15.1^\circ$  and  $19.8^\circ$ . Subsequent to acid hydrolysis of SS, the SSN obtained showed the following changes in its x-ray

diffraction pattern. The peaks at  $15.1^\circ$  ( $\bar{2}20$ ),  $17.8^\circ$  (020) and  $23.1^\circ$  (121) increased in their intensity remarkably. The peaks at  $19.8^\circ$  and  $27.2^\circ$  were appearing more prominently. All these bands indicate a typical pattern of A-type polymorphs, similar to that reported earlier<sup>22</sup>. During acid hydrolysis of SS, the acid attacks amorphous area rapidly than the crystalline region resulting in the formation of SSN which is largely crystalline in nature<sup>23</sup>. The loss of amorphous fraction associated with an increase in the crystalline region is responsible for the increase in the intensity of the peaks in the XRD of SSN<sup>24</sup>.

The XRD patterns of PVA, PVA+10 % SS and PVA+10 % SSN are shown in Fig. 3(b). The degree of crystallinity of all the samples was estimated using the method described by Shujun<sup>25</sup>, *et al.* When PVA is blended with sorghum starch and sorghum starch nanocrystals diffraction peaks  $2\theta$  appears at  $19.3^\circ$  and  $19.7^\circ$ , respectively. The crystallinity and the crystallinity index evaluated for PVA+10 % SS films were 62.8 per cent and 0.58 respectively. In case of PVA+10 % SSN films, intensity of diffraction peaks were increased and the crystallinity and crystallinity index calculated are 65.2 per cent and 0.72 respectively. This clearly indicated that the addition of SSN to PVA has enhanced the crystalline nature of the nano composite film.

### 3.3 Morphological Characterisation

AFM image and 3D image of SSN are given in Figs. 4(a) and 4(b). The particle sizes of the SSN were found to vary from 65 nm - 68 nm. These nanoparticles were used for preparation of PVA nanocomposites. Fig. 4(c) shows the SEM images of sorghum starch. SS granules were found to be spherical in shape which is in agreement with earlier reports<sup>26</sup>. The average particle size is found to be 6  $\mu\text{m}$  - 7  $\mu\text{m}$ .

SEM images of cross section of PVA and its composite films are shown in Figs. 4(d), 4(e), and 4(f). PVA has a relatively smooth surface where as its composites films have shown some particles in their SEM image. The SEM image of PVA nanocomposite seems to have a smoother image and it could be due to smaller size and homogenous distribution of the fillers in the PVA matrix.

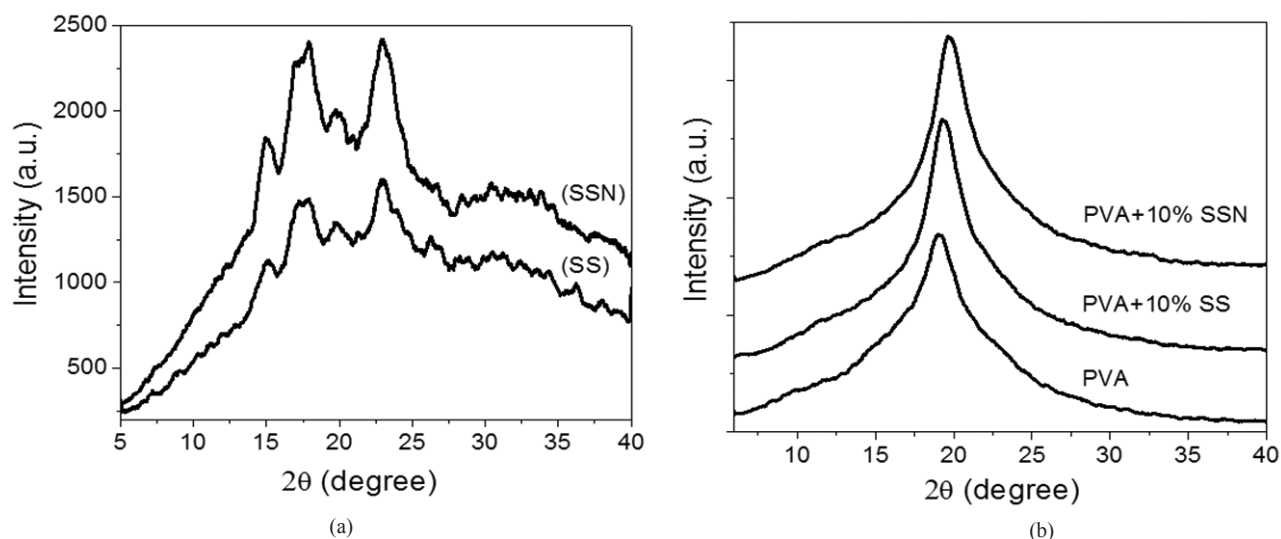


**Figure 3.** X-ray diffractograms of (a) sorghum starch and sorghum starch nanocrystals and (b) PVA and its composites films.



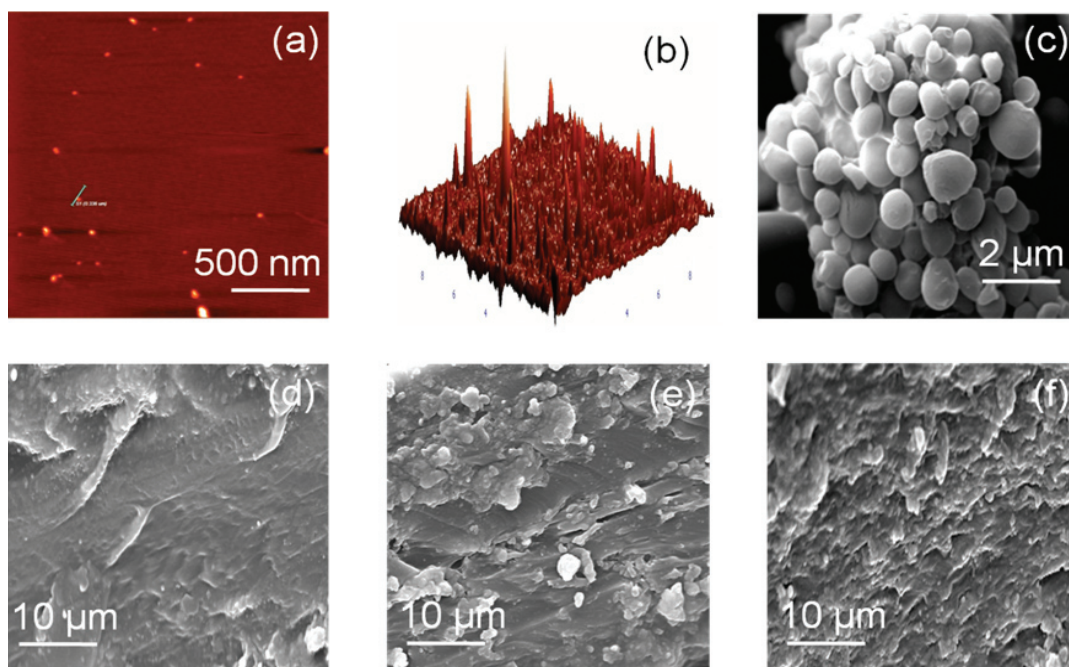


Figure 4. (a) AFM image of SSN (b) 3-D images of SSN (c) SEM images of SS (d) Cross section images of PVA film (e) PVA+10 % SS Film (f) PVA+10 % SSN film.

### 3.4 Physico-mechanical Properties

In Fig. 5, is given the stress v/s strain graph of PVA, PVA+10 % SS and PVA+10 % SSN. In the case of PVA+SS film, with increase in concentration of sorghum starch tensile strength and percentage elongation at break of the films decreased regularly. This can be attributed to excellent mechanical properties of PVA itself and poor compatibility of PVA and the starch. On the other hand, addition of SSN to PVA resulted in an increase in its mechanical properties (tensile strength and percentage strain at break) of the nanocomposite film upto a concentration of 10 per cent of SSN in PVA. Further increase in SSN concentration in PVA+SSN nanocomposite film showed a decrease in its mechanical properties. Chen *et al* has also reported similar observations in the case of PVA pea starch nanocomposites films<sup>14</sup>. The enhancement in the mechanical properties of the polymer nanocomposite (young's modulus, tensile strength and percentage elongation at break), has been attributed to enhanced H-bonding interaction between

the polymer and the starch nanocrystals. These results are supported by FTIR data. The inter molecular interaction can effectively facilitate stress transfer between polymer matrix and the nanocrystals there by transfer the load on the polymer chain to more rigid starch nanocrystals during mechanical stress. Thus, the starch nanocrystals are acting as a load bearing component resulting in improved tensile strength and modulus in the polymer nanocomposites.

It has been observed that with increase in the concentration of SSN beyond certain level, the nanocomposite films tend to decrease its mechanical properties and after a certain concentration of the nanocrystals the mechanical properties of the films decrease below that of PVA. Since the size of SSN is relatively smaller, larger loading of the nanomaterials into PVA matrix is possible and these nanoparticles get more uniformly distributed in a wider area of PVA. This can results in extended H- bonded network with PVA which is responsible for better mechanical properties. As the concentration of the

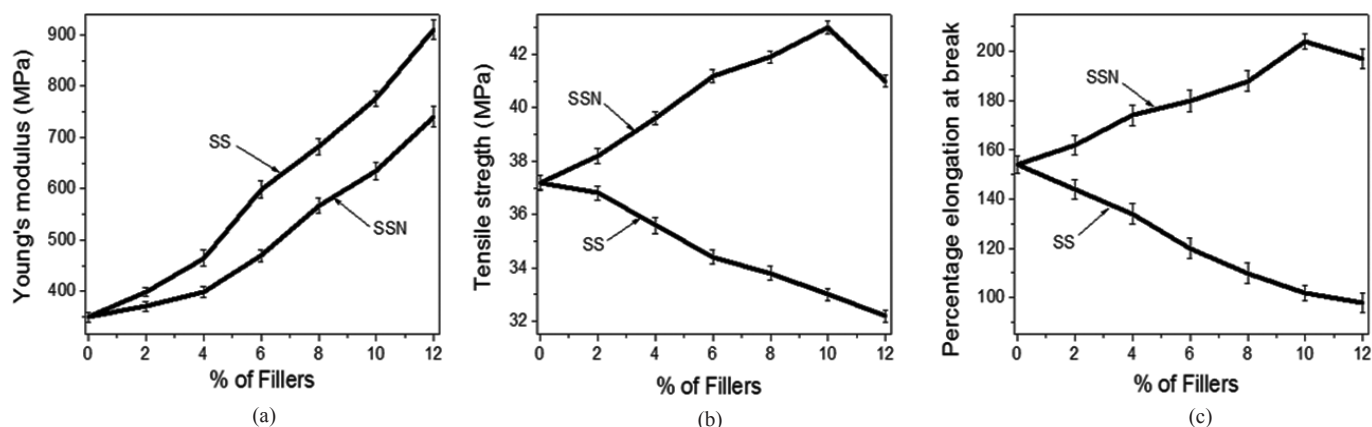


Figure 5. (a) Young's modulus, (b) Tensile strength, and (c) Percentage elongation at break of PVA and its composite films.

nanomaterials in the matrix cross beyond certain limits, further addition of SSN particles results in enhanced proximity of the nanomaterials among themselves, resulting in an increased molecular interactions between themselves. This can lead to agglomeration of the nanoparticles or 3 dimensional networks of self assembled nanocrystals within the system. The formation of such self assembled H-bonded species is evident from the low frequency shift of -O-H stretching vibration of PVA+SSN system for higher concentration of nanomaterials in the nanocomposite films (Table. 1). Thus, the intermolecular H-bonding among starch nanocrystals in the polymer nanocomposite with higher concentration of SSN results in the formation of certain weak points. These weak points tend to undergo fracture with lower strain compared to the PVA matrix alone. The fracture developed can spread cracks along the nanocomposite film as it transfer the load through the nanomaterial to PVA matrix resulting in overall failure of the polymer nanocomposite. This explains the lower percentage of strain at break beyond a certain threshold levels of nanomaterial in the polymer nanocomposites. Similar observations were reported in the case of PVA and bacterial cellulose nanocrystals films<sup>27</sup>. Thus it can be assumed that molecular interactions as well as particle size of nanomaterials play a crucial role in determining the mechanical properties of PVA+SSN nanocomposites.

### 3.5 Differential Scanning Calorimetric Analysis

DSC thermograms of PVA and its composite films are shown in Fig. 6. Glass transition temperatures of PVA, PVA + SS and PVA + SSN were found to be 25.9 °C, 27.4 °C and 30.4 °C respectively. It can be observed that there is a small increase in the glass transition temperature on addition of SS and SSN to PVA. Glass transition temperature ( $T_g$ ) of a polymer nanocomposites is affected by molecular interaction between polymer chains and the additives. In the present case both the polymer and the additives are hydrophilic in nature resulting in a interaction (hydrogen bonding) between them. This leads to a coupling between the -OH groups of PVA and the additive (both SS and SSN). This coupling effect can restrict the segmental mobility of the PVA chains and subsequently

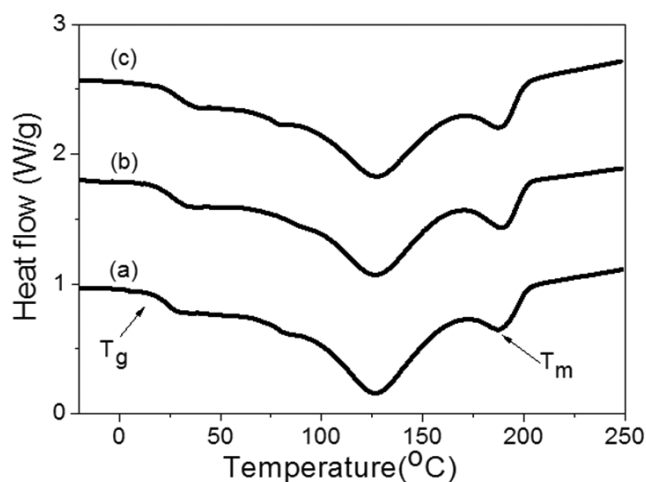


Figure 6. DSC thermograms of (a) PVA film, (b) PVA+10 % SS film, and (c) PVA+10 % SSN film.

increase the  $T_g$ . The extent of such coupling is more pronounced and wide spread in PVA+10 % SSN system, because of smaller size of the nanoparticles and its ability to get dispersed more uniformly in the PVA matrix. The melting temperature of PVA, PVA+10 % SS and PVA+10 % SSN were found to be 188.8 °C, 186.3 °C and 190.0 °C respectively. The corresponding melting enthalpy ( $\Delta H_m$ ) evaluated were found to be 26.2 J/g to 28.6 J/g and 29.2 J/g. The increase in melting enthalpy also points to enhanced molecular interactions resulting in stronger adhesion between PVA and the added filler which demands higher melting enthalpy. These results indicates that polymer - nanocrystals interactions are strong and improving the thermal properties of the nanocomposite films at the temperature range considered.

### 3.6 Thermo Gravimetric Analysis (TGA)

The thermal characteristics of PVA and its nanocomposites were evaluated using TGA and the DTGA curves are shown in Fig. 7. The thermal degradation of these films were measured from 30 °C to 600 °C. The degradation process of PVA can be divided into three phases. The decomposition initially involves dehydration of the hydroxyl groups. This is followed by the formation of volatile organic compounds which subsequently produce conjugated unsaturated polyene structures<sup>28</sup>. As temperature increases above 450 °C, the second stage degradation commences, where low molecular weight compounds such as alkenes, alkanes and aromatics were produced. Above 500 °C carbonaceous residues will be formed. In the present case it can be observed that thermal decomposition temperature of PVA+10 % SS composite film has shifted slightly toward lower temperature compared to PVA. The degradation pattern of PVA+10 % SSN nanocomposites film indicates that there is further reduction in the stability of the nanocomposite at high temperature compared to PVA and PVA+SS system. This indicates that the presence of SS or SSN in the composite film decreases the stability of PVA at high temperature. Thermal degradation of SSN shows that SSN degrades at a relatively lower temperature compared to PVA. Thus the degradation of the additives (SS or SSN) could

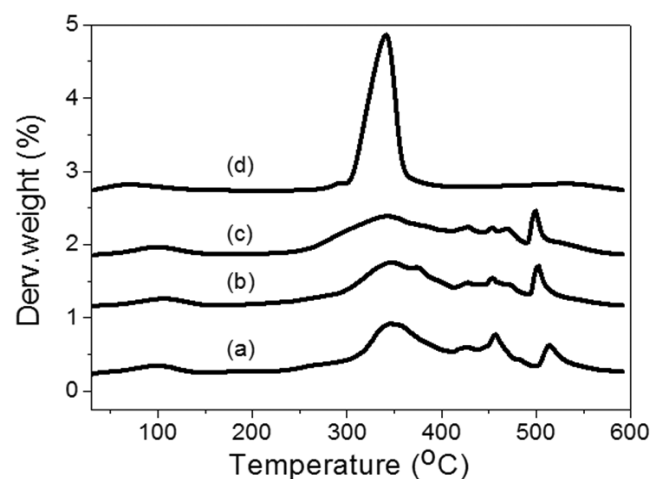


Figure 7. DTGA curves of (a) PVA film, (b) PVA+10 % SS film, (c) PVA+10 % SSN film and (d) Sorghum Starch Nanocrystals.

be responsible for inducing more degradation reactions in PVA composite materials at lower temperature which in turn can reduce the stability of the PVA films at high temperature. Similar observation was reported in PVA and cellulose nanocrystals film<sup>27</sup>.

### 3.7 Dynamic Mechanical Analysis

Dynamic mechanical properties of PVA based nanocomposites were analysed by recording various parameters such as storage modulus and loss tangent as a function of temperature. The results are given in Fig. 8. The storage modulus (Fig. 8(a)) of PVA nanocomposites were found to increase considerably after the incorporation of SS. It further increased when SSN was incorporated in place of SS, as compared to that of pure PVA film. This indicates that the presence of the additives played a predominant role in improving the dynamic mechanical properties of nanocomposite due to the strong interaction between the additive and PVA. The possible formation of a three dimensional network like structure can maximize the stress transfer and contribute to the rise in overall modulus of polymer nanocomposites. The  $\tan \delta$  Vs temperature peaks (Fig. 8(b)) exhibited a substantial change in the maximum temperature ( $T_{max}$ ) on addition of the additives

into PVA. The shift in  $T_{max}$  towards higher temperature with the addition of SS and SSN, indicates an increase in the  $T_g$  values of the nanocomposite systems. This correlates well with the trends observed in the DSC studies. This further proves that the incorporation of nano fillers such as SSN into PVA matrix resulted in decreased segmental mobility, which in turn resulted in an increased  $T_g$ .

### 4. CONCLUSION

Sorghum starch was isolated from sorghum grains. Sorghum starch nanocrystals were prepared from sorghum starch after hydrolysing with sulphuric acid. These materials were used to make PVA composite films by casting and evaporation process. Physico-mechanical properties of PVA + SS composite films, were found to be lower than that of PVA films. However, the same was found to be better for PVA + SSN films.  $T_g$  and dynamic mechanical Properties of PVA nanocomposite were also found to be better than PVA. This could be attributed to the stronger interaction of PVA and SSN because of smaller size of nanoparticles and better homogeneous distribution of it in PVA matrix there by limiting the segmental mobility of PVA. But, TGA studies indicates a slightly lower stability for both PVA + SS and PVA + SSN composite films at very high temperature compared to PVA films. This could be attributed to the faster degradation of the filler/additive itself than PVA making the system less stable at substantially high temperatures.

### REFERENCES

- Hallensleben, M.L.; Fuss, R. & Mummy, F. Polyvinyl compounds, others. Ullmann's encyclopedia of industrial chemistry. Wiley - VCH online library, 2015. doi: 10.1002/14356007.a21\_743.pub2
- Paradossi, G.; Cavalieri, F.; Chiessi, E.; Spagnoli, C. & Cowman, M.K. Poly(vinyl alcohol) as versatile biomaterial for potential biomedical applications. *J. Mater. Sci. Med.*, 2003, **14**(8), 687-691.
- Follain, N.; Joly, C.; Dole, P. & Bliard, C. Properties of starch based blends. Part 2. Influence of Polyvinyl alcohol addition and photocrosslinking on starch based materials mechanical properties. *Carbohydr. Polym.*, 2005, **60**(2), 185-192. doi: 10.1016/j.carbpol.2004.12.003
- Siddaramaiah; Raj, B. & Somashekar, R. Structure-property relation in polyvinyl alcohol/starch composites. *J. Appl. Polym. Sci.*, 2004, **91**(1), 630-635. doi: 10.1002/app.13194
- Lu, J.; Wang, T. & Drzal, L.T. Preparation and properties of microfibrillated cellulose polyvinyl alcohol composite materials. *Compo. Part A: Appl. Sci. Manufact.*, 2008, **39**(5), 738-746. doi: 10.1016/j.compositesa.2008.02.003
- Jia, Y.T.; Gong, J.; Gu, X.H.; Kim, H.Y.; Dong, J. & Shen, X.Y. Fabrication and characterization of poly(vinyl alcohol)/chitosan blend nanofibers produced by electrospinning method. *Carbohydr. Polym.*, 2007, **67**(3), 403-409. doi: 10.1016/j.carbpol.2006.06.010

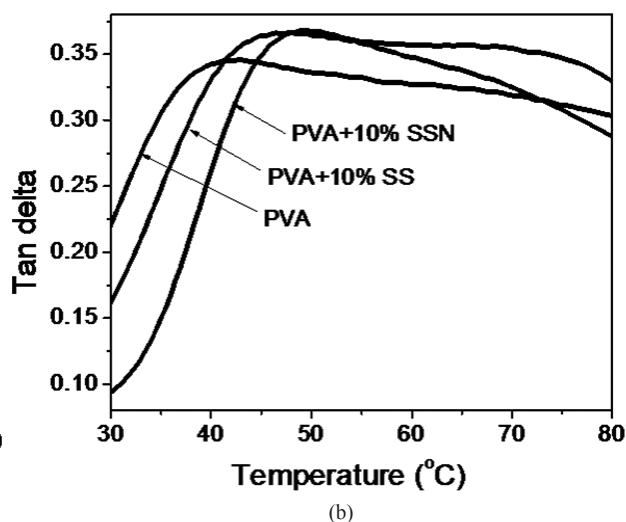
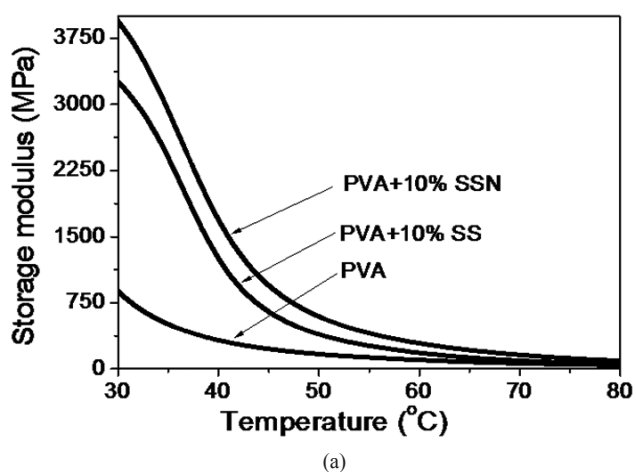


Figure 8. DMA thermograms (a) Storage modulus and (b) Tan delta of PVA and its composite films.



7. Su, J.F.; Huang, Z.; Liu, K.; Fu, L.L. & Liu, H. R. Mechanical properties, biodegradation and water vapor permeability of blend films of soy protein isolate and poly (vinyl alcohol) compatibilized by glycerol. *Polym. Bullet.*, 2007, **58**(5), 913-921.  
doi: 10.1007/s00289-007-0731-7
8. Manias, E. Nanocomposites - Stiffer by design. *Nature Mater.*, 2007, **6**, 9-11.  
doi:10.1038/nmat1812
9. Yang, Z.; Xu, D.; Liu, J.; Liu, J.; Li, L.; Zhang, L., & Lv, J. Fabrication and characterization of poly(vinyl alcohol)/carbon nanotube melt-spinning composites fiber. *Progr. Natu. Sci. Mater. Inter.*, 2015, **25**(5), 437-444.  
doi: 10.1016/j.pnsc.2015.09.014
10. Bao, C.; Guo, Y.; Song, L. & Hu, Y. Poly (vinyl alcohol) nanocomposites based on graphene and graphite oxide: A comparative investigation of property and mechanism. *J. Mater. Chem.*, 2011, **21**(36), 13942-13950.  
doi: 10.1039/C1JM11662B
11. Paiva, M.C.; Zhou, B.; Fernando, K.A.S.; Lin, Y.; Kennedy, J.M. & Sun, Y.P. Mechanical and morphological characterization of polymer-carbon nanocomposites from functionalized carbon nanotubes. *Carbon*, 2004, **42**(14), 2849-2854.  
doi: 10.1016/j.carbon.2004.06.031
12. Yu, Y.H.; Lin, C.Y.; Yeh, J.M. & Lin, W.H. Preparation and properties of poly (vinyl alcohol)-clay nanocomposite materials. *Polymer*, 2003, **44**(12), 3553-3560.  
doi: 10.1016/S0032-3861(03)00062-4
13. Andreas, A. Sapalidis.; Fotios, K. Katsaros & Nick, K. Kanellopoulos. PVA / Montmorillonite Nanocomposites: Development and properties. *In Nanocomposites and Polymers with Analytical Methods*, Dr. John Cuppoletti (Ed.), InTech 2011.  
doi: 10.5772/18217
14. Chen, Y.; Cao, X.; Chang, P.R. & Huneault, M.A. Comparative study on the films of poly (vinyl alcohol)/pea starch nanocrystals and poly (vinyl alcohol)/native pea starch. *Carbohydr. Polym.*, 2008, **73**(1), 8-17.  
doi: 10.1016/j.carbpol.2007.10.015
15. Silverio, H.A.; Neto, W.P.F. & Pasquini, D. Effect of incorporating cellulose nanocrystals from corncob on the tensile, thermal and barrier properties of poly (vinyl alcohol) nanocomposites. *J. Nanomater.*, 2013, 1-9.  
doi: 10.1155/2013/289641
16. Beta, T.; Chisi, M. & Monyo, E.S. Sorghum/harvest, storage, and transport in encyclopedia of grain science, edited by C. W. Wrigley, H. Corke, C. E. Walker, Elsevier, Oxford, 2004.
17. Waniska, R.D.; Rooney, L.W. & McDonough, C.M. Sorghum/utilization in encyclopedia of grain science, edited by C. W. Wrigley, H. Corke, C. E. Walker, Elsevier, Oxford, 2004.
18. Zhu, F. Structure, physicochemical properties, modifications, and uses of sorghum starch. *Compr. Rev. Food. Sci. Food. Saf.*, 2014, **13**(4), 597-610.  
doi: 10.1111/1541-4337.12070
19. Ai, Y.F.; Medic, J.; Jiang, H.X.; Wang, D.H. & Jane, J.L. Starch characterization and ethanol production of sorghum. *J. Agric. Food. Chem.*, 2011, **59**(13), 7385-7392.  
doi: 10.1021/jf2007584
20. Udachan.; Iranna, S.; Sahoo A.K. & Hend, G.M. Extraction and characterization of sorghum (*Sorghum bicolor* L. Moench) starch. *Int. Food. Res. J.*, 2012, **19**(1), 315-319.
21. Angellier, H.; Choisnard, L.; Molina-Boisseau, S.; Ozil, P. & Dufresne, A. Optimization of the preparation of aqueous suspensions of waxy maize starch nanocrystals using a response surface methodology. *Biomacromolecules.*, 2004, **5**(4), 1545-1551.  
doi: 10.1021/bm049914u
22. Xu, Y.; Sismour, E.N.; Grizzard, C.; Thomas, M.; Pestov, D.; Huba, Z.; Wang, T. & Bhardwaj, H.L. Morphological, structural and thermal properties of starch nanocrystals affected by different botanic origins. *Cer. Chem.*, 2014, **91**, 383-388.  
doi: 10.1094/CCHEM-10-13-0222-R
23. Putaux, J.; Molina-Boisseau, S.; Momaur, T. & Dufresne, A. Platelet nanocrystals resulting from the disruption of waxy maize starch granules by acid hydrolysis. *Biomacromolecules*, 2003, **4**, 1198-1202.  
doi: 10.1021/bm0340422
24. Puchongkavarin, H.; Bergthaller, W.; Shobsngob, S. & Varavinit, S. Characterization and utilization of acid-modified rice starches for use in pharmaceutical tablet compression. *Starch/Starke*, 2003, **55**, 464-475.  
doi: 10.1002/star.200300232
25. Shujun, W.; Jinglin, Y. & Wenyuan, G. Use of x-ray diffractometry (xrd) for identification of fritillaria according to geographical origin. *Am. J. Biochem. Biotech.*, 2005, **1**, 199-203.
26. Vallons, K.J.R. & Arendt, E.K. Effects of high pressure and temperature on the structural and rheological properties of sorghum starch. *Inno. Food. Sci. & Emerg. Tech.*, 2009, **10**(4), 449-456.  
doi: 10.1016/j.ifset.2009.06.008
27. George, J.; Sajeevkumar, V.A.; Ramana, K.V.; Sabapathy, S.N. & Siddaramaiah. Augmented properties of PVA hybrid nanocomposites containing cellulose nanocrystals and silver nanoparticles. *J. Mater. Chem.*, 2012, **22**(42), 22433-22439.  
doi: 10.1039/C2JM35235D
28. Tubbs, R.K. & Ting, K.W. Thermal properties of polyvinyl alcohol. John Wiley, Chichester, 1973.

#### ACKNOWLEDGEMENTS

The authors thank Dr Rakesh Kumar Sharma, Director DFRL, Mysuru for his support and encouragement. The authors are also thankful to Dr S.N. Sabapathi, Head (Food Engineering and Packaging) and other staff of the division for constant motivation and help.



## CONTRIBUTORS

**Mr S. Vasantha Kumar** is a research scholar working in Food Engineering and Packaging Department at Defence Food Research Laboratory Mysuru.

He was involved in isolation of sorghum starch as well as sorghum starch nanocrystals, preparation of all PVA composite films and most of the analysis like physicochemical properties, AFM, XRD, Thermal analysis, etc

**Dr V.A. Sajeevkumar** received his PhD in Chemistry and currently working as Scientist 'F' in Food Engineering and Packaging Department at Defence Food Research Laboratory Mysuru.

He has initiated the work on development of the nanocomposite films of PVA with natural fillers, planned the experiments carried out FTIR characterisation and contributed towards the interpretation of results, drafting and revision of manuscript.

**Dr Johnsy George** received his PhD in Polymer Science and currently working as Scientist 'E' in Food Engineering and Packaging Department at Defence Food Research Laboratory Mysuru.

He was involved in the conduct of experiments using DMA and interpretation of its results.

**Mr Sunny Kumar** is Senior Technical Assistant 'B' working in Food Engineering and Packaging Department at Defence Food Research Laboratory Mysuru.

He was involved in morphological characterisation of sorghum starch as well as PVA composites films using scanning electron microscope.